



# Density and viscosity of liquid ZrO<sub>2</sub> measured by aerodynamic levitation technique



Toshiki Kondo<sup>a</sup>, Hiroaki Muta<sup>a</sup>, Ken Kurosaki<sup>a</sup>, Florian Kargl<sup>b</sup>, Akifumi Yamaji<sup>c</sup>, Masahiro Furuya<sup>d</sup>, Yuji Ohishi<sup>a,\*</sup>

<sup>a</sup> Graduate School of Engineering, Osaka University, Japan

<sup>b</sup> Institut für Materialphysik im Weltraum, Deutsches Zentrum für Luft – und Raumfahrt (DLR), 51170, Köln, Germany

<sup>c</sup> Graduate School of Advanced Science and Engineering, Waseda University, Japan

<sup>d</sup> Central Research Institute of Electric Power Industry, Japan

## ARTICLE INFO

### Keywords:

Materials science

ZrO<sub>2</sub>

Aerodynamic levitation

Viscosity

Density

Liquid phase

Severe accident

## ABSTRACT

Liquid ZrO<sub>2</sub> is one of the most important materials involved in severe accident analysis of a light-water reactor. Despite its importance, the physical properties of liquid ZrO<sub>2</sub> are scarcely reported. In particular, there are no experimental reports on the viscosity of liquid ZrO<sub>2</sub>. This is mainly due to the technical difficulties involved in the measurement of thermo-physical properties of liquid ZrO<sub>2</sub>, which has an extremely high melting point. To address this problem, an aerodynamic levitation technique was used in this study. The density of liquid ZrO<sub>2</sub> was calculated from its mass and volume, estimated based on the recorded image of the sample. The viscosity was measured by a droplet oscillation technique. The density and viscosity of liquid ZrO<sub>2</sub> at temperatures ranging from 2753 K to 3273 K, and 3170 K–3471 K, respectively, were successfully evaluated. The density of liquid ZrO<sub>2</sub> was found to be 4.7 g/cm<sup>3</sup> at its melting point of 2988 K and decreased linearly with increasing temperature, and the viscosity of liquid ZrO<sub>2</sub> was 13 mPa at its melting point.

## 1. Introduction

To predict the progression of a core melt-down accident of a light-water reactor, it is necessary to understand the physical behavior of the molten core materials: how they flow down the core region, how they breach the pressure vessel and eject, and how they spread at the bottom of the containment vessel. An accurate understanding of the behavior of the molten core materials is one of the key issues to predict the distribution of the fuel debris, which is one of the most important issues for the defueling operation in the Fukushima Daiichi (1F) nuclear power plant. For such prediction, advanced computer simulation methods, such as the moving particle semi-implicit (MPS) method, are being developed, which directly simulates molten core behavior by discretizing the governing equations [1]. To get reliable data from such computer simulations, accurate physical properties of molten corium are required as initial input parameters. Viscosity is a key physical property to predict the flow behavior of melts.

In the early stage of the accident, a metallic liquid phase is generated from zircaloy (Zr-based alloy), stainless steel (Fe-, Ni-, and Cr-based alloy), and B<sub>4</sub>C. The physical properties of Zr–Fe [2], Zr–Ni and Zr–Cr

[3] liquid alloys have been reported. When the temperature of the fuels exceeds 2300 K, zircaloy claddings will react with UO<sub>2</sub> fuels, resulting in the formation of a U–Zr–O liquid phase. To gain insight into the physical properties of U–Zr–O liquid, this study focuses on liquid ZrO<sub>2</sub>.

Molten ZrO<sub>2</sub> has attracted much attention, not only as a component of the molten core materials, but also as a representative non-glass former. Although the mechanism of the glass-formation ability is not yet fully understood, it is known that glass-formation ability is closely related to the viscosity. Kohara et al [4] performed X-ray diffraction measurement on liquid ZrO<sub>2</sub> using synchrotron radiation. They reported that Zr–O bonds in liquid ZrO<sub>2</sub> have short lifetimes, which explains the low viscosity (~2 mPa at 3073 K calculated by combined density functional theory and molecular dynamics simulations) and potentially also the low glass-formation ability of liquid ZrO<sub>2</sub>.

Despite the high interest in thermophysical properties, there are to our knowledge no experimentally obtained data on the viscosity of molten ZrO<sub>2</sub> reported because of the difficulty to carry out such measurements caused by the materials high melting temperature (2988 K [5]). Due to melt-container reaction conventional container-based techniques cannot be applied. This problem can be solved by using levitation

\* Corresponding author.

E-mail address: [ohishi@see.eng.osaka-u.ac.jp](mailto:ohishi@see.eng.osaka-u.ac.jp) (Y. Ohishi).

<https://doi.org/10.1016/j.heliyon.2019.e02049>

Received 29 December 2018; Received in revised form 13 May 2019; Accepted 3 July 2019

2405-8440/© 2019 The Author(s). Published by Elsevier Ltd. This is an open access article under the CC BY-NC-ND license (<http://creativecommons.org/licenses/by-nc-nd/4.0/>).

techniques. Amongst the different levitation techniques, aerodynamic levitation (ADL) is the most appropriate technique for the levitation of oxides [6]. In this technique, a sample is levitated by a gas flow using a conical nozzle. Therefore, reduction of the sample can be easily prevented by mixing oxygen into the flowing gas. Recently, Langstaff et al. developed a new method to evaluate the viscosity of the liquid sample levitated by ADL [7]. In this method, the viscosity is evaluated from the damping constant of droplet oscillation that are precisely induced by a pressure wave in the gas flow using loud-speakers operated at the droplet oscillation resonance frequency. The viscosities of molten  $\text{Al}_2\text{O}_3\text{-ZrO}_2$  mixtures have already been evaluated by this method [8]. The present study reports the experimentally obtained viscosity of liquid  $\text{ZrO}_2$ , which has the highest melting temperature among the materials that had their viscosity measured by ADL, for the first time.

## 2. Experimental

The sample was aerodynamically levitated in a convergent-divergent conical nozzle and melted by lasers. The density of the liquid sample was calculated from its known mass and the measured volume, which was evaluated from the recorded images of the sample. The viscosity was measured by the droplet oscillation technique. This method measures the viscosity by observing the damping behavior of the oscillated samples. Fig. 1 shows the schematic view of the ADL furnace used for the measurement. This furnace was built in reference to the one developed at the German Aerospace Center (DLR) [9] based on the Aberystwyth University design by Langstaff et al. [6]. This ADL furnace comprises a levitation system, a heating system, an image-recording system, and a droplet oscillation system.

### 2.1. Levitation and heating system

The levitation system consists of a conical converging-diverging

nozzle (diameter: converging part is 1mm, and diverging part is 3 mm) and a levitation gas supplying system. Approximately 15%  $\text{O}_2$  and 85% Ar mixture gas was supplied to the nozzle using a mass flow-controller at a typical combined flow rate of  $400 \text{ cm}^3 \text{ min}^{-1}$ .  $\text{O}_2$  was added to prevent the reduction of samples during the experiments. The color of all the samples used in this study was white after the experiments, suggesting that the samples were not reduced. The sample was levitated by the gas flowing through the nozzle. The levitated sample was melted by two 100-W  $\text{CO}_2$  lasers (Coherent, GEM100) emitting at approximately  $10.6 \mu\text{m}$ . One laser was aimed at the top of the sample, and the other was aimed at the bottom of the sample to prevent a temperature gradient between the bottom and the top of the sample.

The temperature of the sample was measured using a single-color ( $0.9 \mu\text{m}$ ) pyrometer (Chino, IR-CAS8CNL). The data were recorded every 2 ms by a data logger (Graphtec, GL-900). Because the emissivity of liquid  $\text{ZrO}_2$  is not known, we calibrated the temperature measured by the pyrometer ( $T_p$ ) to the real temperature ( $T$ ) of the samples based on Wien's law [10].

$$\frac{1}{T} - \frac{1}{T_p} = \frac{1}{T_L} - \frac{1}{T_{LP}} \quad (1)$$

where  $T_L$  is the melting point, and  $T_{LP}$  is the melting point measured by the pyrometer all in units of Kelvin. The value of  $T_L$  used for liquid  $\text{ZrO}_2$  was 2988 K [5], and that of  $T_{LP}$  was determined based on the cooling curve corresponding to the maximum of recalescence, shown in Fig. 2. To apply this equation, it is assumed that emissivity of the sample does not change in the temperature range of interest. Therefore, it must be noted that the uncertainty in the calibrated temperature would increase with increasing temperature.

### 2.2. Image-recording system

Images of the levitated sample were recorded using a high-speed

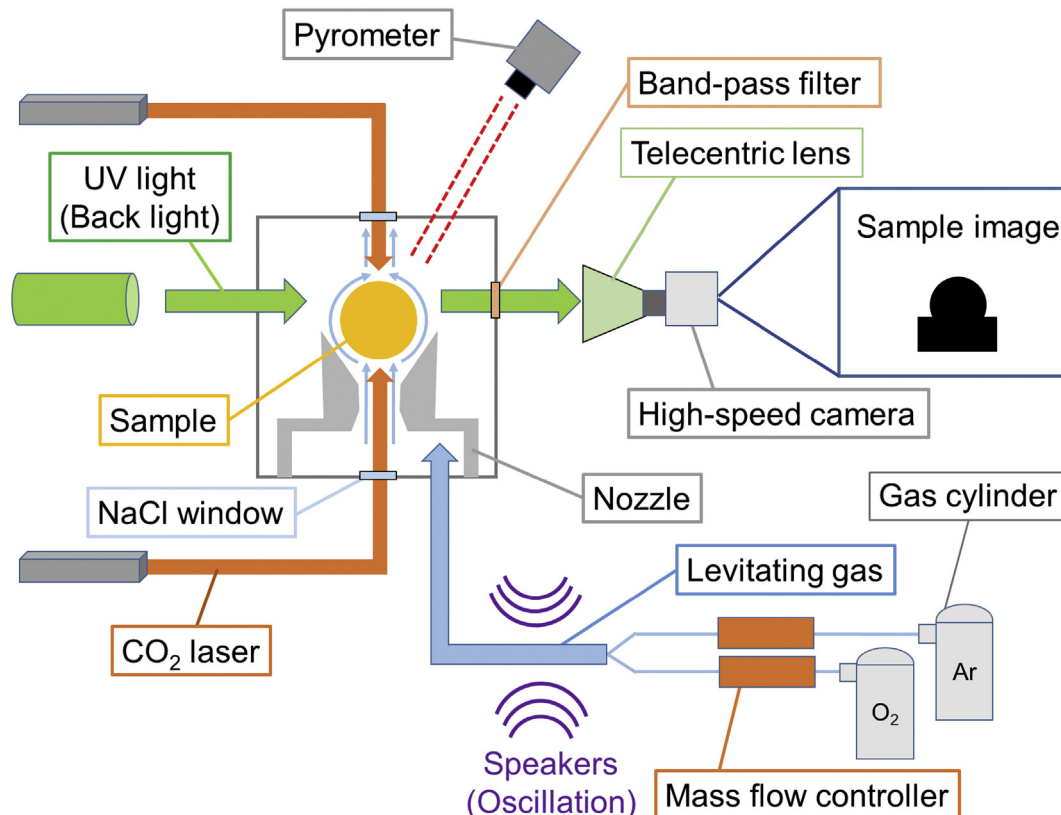


Fig. 1. Schematic view of the aerodynamic levitation apparatus.

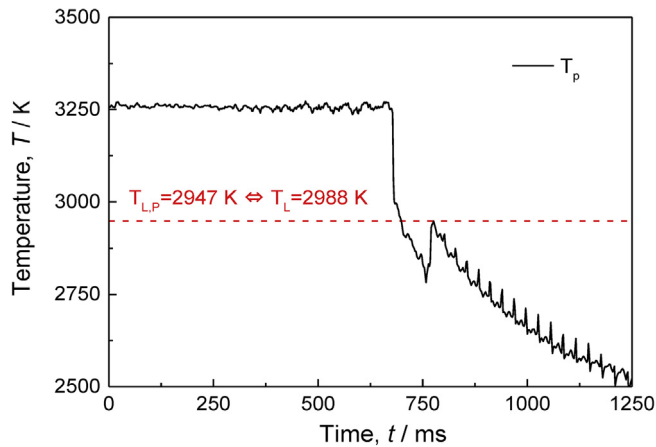


Fig. 2. Cooling curve of the  $ZrO_2$  during the experiment.

camera (Ditect, HAS-D72M) equipped with a telecentric lens (Edmund, TS GOLD). The frame rate of the high-speed camera was 2000 fps. UV light was used as a back light (Hamamatsu, Ls9588-02A) with a  $370 \pm 2$  nm bandpass filter. Because the lower part of each sample was hidden by the edge of the conical nozzle, it was only partially visible. Thus, the visible part was fitted by an ellipsoid to estimate the whole shape of the sample. Fig. 3(a) shows the image of liquid  $ZrO_2$  taken by the high-speed camera. The edge was extracted and fitted as shown in Fig. 3(b). The horizontal and vertical diameters of the sample were output in pixels. To convert pixels into millimeters, steel use stainless (SUS) balls with diameters of 2.0 mm–3.0 mm were measured. The deviation of the diameter measured by micrometer calliper (Mitsutoyo, MPC-25MX) of each SUS ball was less than 0.008 mm Fig. 4 shows the relationship between pixel number and the diameter of the SUS balls. From this result, a conversion relationship of 1 pixel =  $5.8 \times 10^{-3}$  mm was obtained and used for further calculation.

### 2.3. Droplet oscillation system

Droplet oscillation was induced by two speakers (Tympany, P830970). The signals fed into the speakers were in the form of a sine wave generated by function generator (AS ONE, AWG1005) and amplified by an amplifier (Pioneer, A-10). The speakers were placed in the gas-supplying system to oscillate the sample by the levitation gas flow. Hereby, the observed oscillation mode of the sample depended on the induced frequency. For viscosity measurements, a vibration mode where vertical and horizontal motions are phase shifted by  $90^\circ$  ( $l = 2$ ,  $m = 0$  mode) must be induced [7]. Therefore, the sample oscillation was visually observed through the camera whilst changing the induced frequency to select the adequate vibrational mode. For the measurement after exciting the sample with the appropriate resonance frequency, after turning off the speakers, the oscillation was damped by viscous friction.

### 2.4. Density and viscosity measurement

The density of the sample ( $\rho$ ) can be calculated from the mass ( $m$ ) and volume ( $V$ ) of the sample by

$$\rho = \frac{m}{V} \quad (2)$$

whereby  $V$  was determined from the recorded images and  $m$  was measured after the ADL experiment. The volume of the sample  $V$  was calculated from the horizontal and vertical diameters of the sample taken from the image analysis, which were recorded after the heating lasers were turned off. The equation of  $V$  is described as

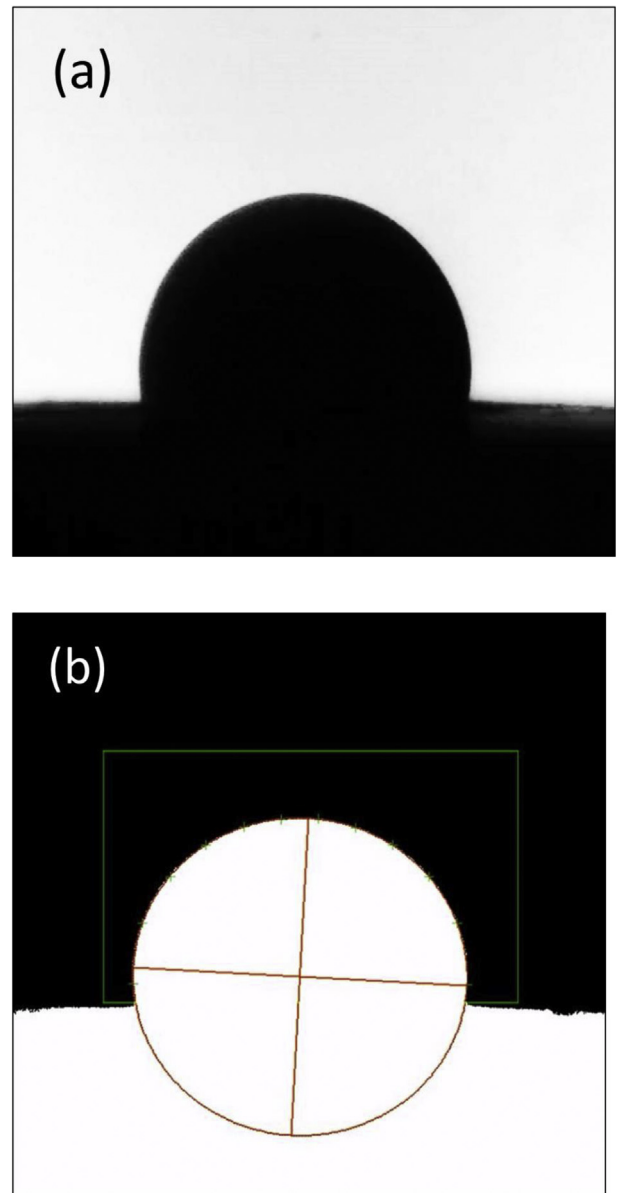


Fig. 3. Images of the levitated sample: (a) taken by the high-speed camera and (b) after binarization for the analysis by the ellipse-fitting program. The red circle marks the fitted ellipse, with the respective minor and major axis represented by the two straight lines.

$$V = \frac{4\pi r_M^2 r_m}{3} \quad (3)$$

whereby  $r_M$  and  $r_m$  are half the major and minor axis, respectively. It is assumed that the sample is symmetric about the minor axis because the rotation of the sample during the experiment was occurred this direction from the analysis of camera images.

The viscosity was determined by applying the oscillation droplet method [11]. In this method, the viscosity ( $\eta$ ) of the sample is calculated from the decay time ( $\tau$ ) of the damped oscillation of the  $l = 2$  mode by

$$\eta = \frac{\rho r_0^2}{5\tau} \quad (4)$$

where  $r_0$  is the radius of the spherical sample, which is calculated from the volume of the sample. The decay time is obtained from the time-dependent diameter of the sample recorded for the damped oscillation of the sample. As an example, the time-dependent horizontal diameter of

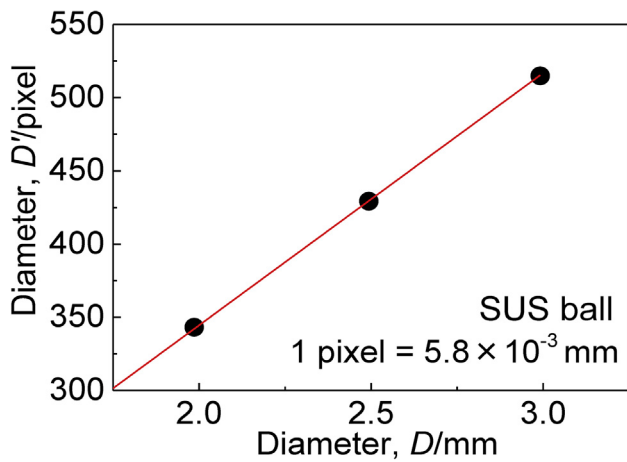


Fig. 4. Pixel to length calibration curve as obtained from the image analysis of SUS reference balls.

liquid  $ZrO_2$  is shown in Fig. 5. The data were fitted by the following damped-harmonic oscillator solution [7].

$$r_h = A \exp\left(-\frac{t-t_1}{\tau}\right) \sin(2\pi\nu_R(t-t_0)) + R_{av} \quad (5)$$

where  $r_h$  is the horizontal or vertical radius of the sample,  $t$  is the time,  $A$  is the initial amplitude,  $t_0$  is an offset time for the oscillation,  $t_1$  is the time the decay starts,  $\nu_R$  is the resonance frequency of the droplet, and  $R_{av}$  is the radius of the droplet at rest. Among them,  $A$ ,  $t_0$ ,  $t_1$ ,  $\nu_R$  and  $R_{av}$  are free parameters and determined by fitting. The coefficient of determination ( $R^2$ ) was higher than 0.98 for all the fittings, which shows that the data were well fitted by Eq. (5). In this equation, the exponential term represents the damping of the oscillations. In this study, the horizontal radius alone was used for the calculation, because the lower part of the sample was not visible; this might have resulted in less reliability of the vertical radius. The decay time was derived from this fitting, and the viscosity was calculated by Eq. (4).

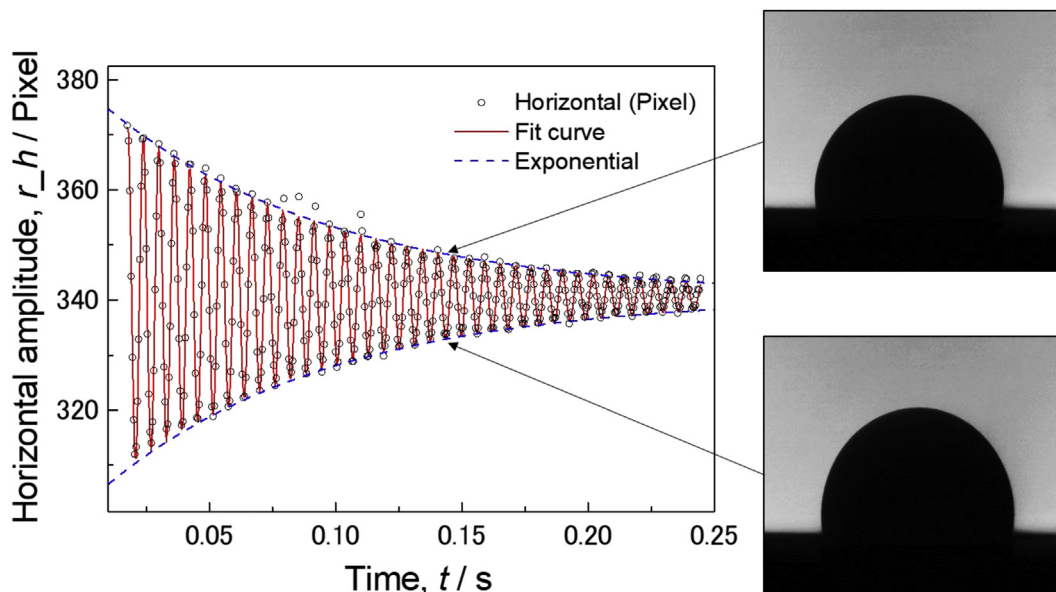


Fig. 5. Left: Time-dependent horizontal amplitude of the decaying droplet oscillation of a  $ZrO_2$  sample. The red curve represents the fit using Eq. (4). Right: The recorded images at the inflection points of the oscillation clearly show the  $l = 2$  mode character of the oscillation.

## 2.5. Sample preparation

Spherical samples with a diameter of approximately 2 mm were used for the ADL experiments.  $ZrO_2$  and  $Al_2O_3$  samples were prepared.  $Al_2O_3$  was measured to evaluate the accuracy of the measurement system by comparing the measured data with literature values. Alumina powder (Kojundo Chemical Lab., 4N) was pressed into a pellet at a pressure of 100 MPa. The pellet was sintered at 1773 K for 12 h in air.  $ZrO_2$  powder (Furuuchi Chemical Lab., 4N, except for Hf impurities—the Hf content was 1.3 wt%) was sintered into a pellet by the spark plasma sintering (SPS) method (Sumitomo Coal Mining Co., Ltd., 511S) at a pressure of 100 MPa at 1723 K in an Ar flow atmosphere. Because SPS was performed in a reducing atmosphere, the color of the sintered  $ZrO_2$  pellet was gray. To compensate the reduced oxygen, the  $ZrO_2$  pellet was heated at 1323 K for 12 h in air, which changed the color of the pellet from gray to white. After sintering, each pellet was crushed and, from the fragments, small pieces with approximately 20 mg weight were selected for the ADL experiments. Once they were melted by laser radiation, they became ellipsoid because of the surface tension.

## 3. Results and discussion

### 3.1. Reference measurement of density and viscosity of liquid- $Al_2O_3$

Fig. 6 shows the temperature-dependent density of the liquid  $Al_2O_3$  with the reference data measured by Langstaff et al. using ADL [7], Tamaru et al. using ESL [12], Paradis et al. using ESL [13], and Kirshenbaum using the Archimedeian method [14]. The data by Tamaru et al. were measured in the International Space Station. Our measured data are almost identical with those of Langstaff [7], whose measurement method was the same as the one in this study. The maximum difference between our data and Langstaff's data is, at most, 1.2% at 1928 K. The ESL data by Paradis are slightly higher than the data in this study, possibly because of the sample reduction and or evaporation during the ESL measurement, because the ESL experiment was conducted under vacuum conditions. The Archimedeian method has been used for a long time as the common technique to measure the density of liquids. However, it is difficult to take measurements at a high temperature, because the sample may react with the vessel during the measurement.

Fig. 7 shows the result of the viscosity measurement for  $Al_2O_3$  with

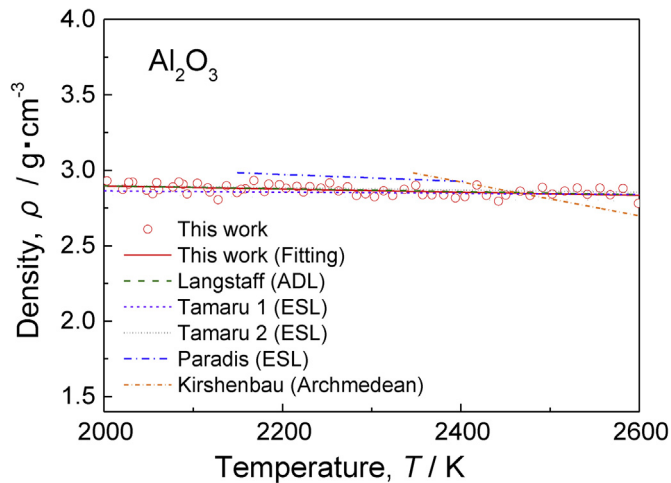


Fig. 6. Density of liquid alumina as function of temperature. Data of this work (red/white bullets) are compared with the results by Langstaff et al. [6] (green dashed line).

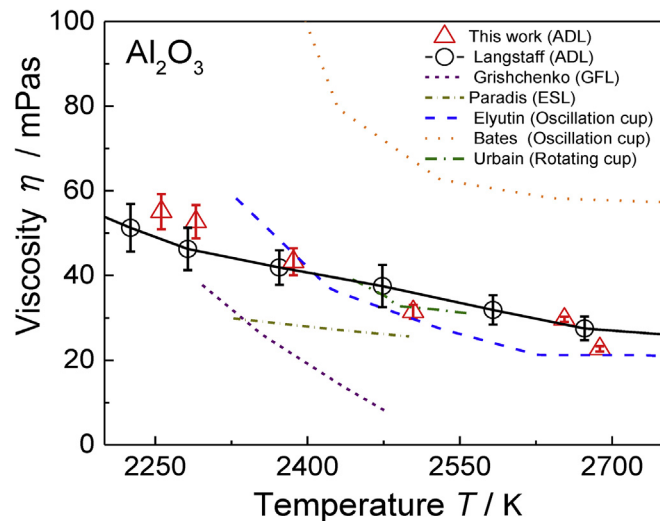


Fig. 7. Viscosity of liquid alumina as a function of temperature. Data of this work (red triangles) are compared with the results of Langstaff et al. [6].

the reference value measured by Langstaff (ADL) [7], Paradis (ESL) [15], Elyutin and Bates (oscillating cup method) [16, 17], Urbain (rotating cup method) [18], and Grishchenko (gas-film levitation, GFL) [19]. Viscosity was measured three times at each temperature, and the standard errors are shown as the error bars in Fig. 7. The literature values significantly differ, suggesting the difficulty in the viscosity measurement of high-temperature liquid  $\text{Al}_2\text{O}_3$ . Among the literature data, the data of this study are in good agreement with those of Langstaff measured by ADL, which is the same method as applied here. The maximum difference between the present data and Langstaff's data is, at most, 18% at 2688 K and within the error bars for this technique. In summary,  $\text{Al}_2\text{O}_3$  measurement revealed with differences between the present and Langstaff's ADL reference data within the error bars, that the present ADL gives accurate results on both of those properties.

### 3.2. Density and viscosity of $\text{ZrO}_2$

The measured density of  $\text{ZrO}_2$  is shown in Fig. 8 together with literature experimental data (taken from the supplemental information of Ref. [4]) and the estimated value [20, 21, 22]. We measured two times (#1 and #2) using different samples, and both data agree within error

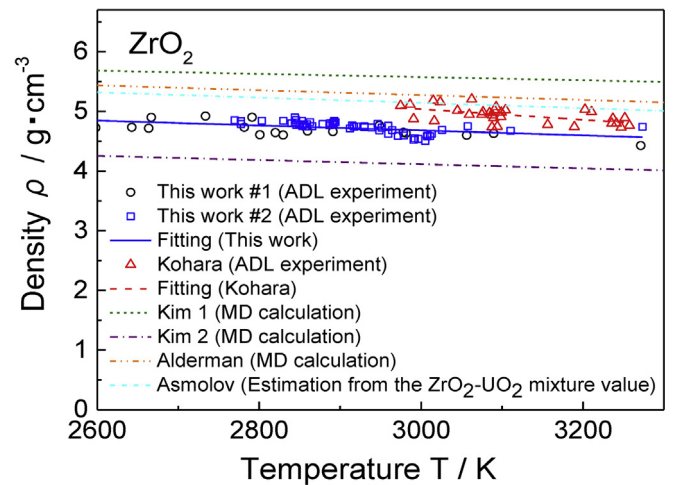


Fig. 8. Temperature dependent density of liquid zirconia determined in two independent runs (open symbols) shown with a fit to the data (blue line) applying Eq. (5) compared with the data of Kohara (red dashed line).

bars. The data are slightly lower than those reported by Kohara et al [4]. Kohara also used the ADL method to measure the density of liquid  $\text{ZrO}_2$ . However, the experimental setup was slightly different from the one in the present research. Kohara et al. only heated the top side of the sample by a single laser. The bottom side was not directly heated. It is known that in ADL without heating from the bottom temperature gradients of several ten to even a few hundred Kelvin are expected [23]. With the temperature measured using a pyrometer focusing on the top side of the sample, they might have overestimated the temperature of the sample. Moreover, the temperature gradient would also lead to a density gradient within the sample. The density of liquid  $\text{ZrO}_2$  decreases linearly with increasing temperature, which is a generally observed behavior for liquids. The recorded densities were described by the following equation [24]:

$$\rho = a(T - T_m) + \rho_m \quad (6)$$

where  $T_m$  is the melting temperature (2988 K for  $\text{ZrO}_2$ ),  $\rho_m$  is the density at the melting temperature, and  $a$  is the free parameter. By fitting this equation to the data in this study, the following equation is obtained

$$\rho_{l-\text{ZrO}_2} = -(4.10 \pm 0.87) \times 10^{-4} (T - 2988) + (4.69 \pm 0.23) \text{ (g/cm}^3\text{)} \quad (2753 \text{ K} < T < 3273 \text{ K}) \quad (7)$$

where  $\rho_{l-\text{ZrO}_2}$  is the density of liquid  $\text{ZrO}_2$ . The density at the melting point is found to be  $4.7 \text{ g/cm}^3$  using Eq. (7).

Although the density measurement finishes in a short period of time (within around 30 s), the viscosity measurement takes a while (about 10 min), because it is necessary to find the appropriate frequency and amplitude of the oscillation for the measurement. Because the vapor pressure of  $\text{ZrO}_2$  is higher than that of  $\text{Al}_2\text{O}_3$  (18 Pa for  $\text{ZrO}_2$  and 0.12 Pa for  $\text{Al}_2\text{O}_3$  at their melting points, calculated using the FACT 53 database), special attention should be paid to the viscosity measurement of liquid  $\text{ZrO}_2$ . To avoid the effect of sample evaporation on the measured results, the viscosity measurement was performed only one time at a certain temperature for one  $\text{ZrO}_2$  sample. To check for evaporation, the mass of the samples was measured before and after the ADL experiments. The change in sample mass during the whole experiment (about 1 min) was less than 7%. This includes the time for adjusting the flow rate of levitating gas, resonant frequency from the speaker, and so on. The actual mass reduction during the density and viscosity measurement is about 0.02% and 0.5%, respectively, because the actual experimental time is about 100 ms for density measurement (the time of sample cooling after laser is switched off) and 2.5 s for viscosity measurement (the time from

turning off the speaker until sample cooling). This means the sample evaporation effect roughly results in a 0.02% overestimation in density measurement and a 0.2% overestimation in viscosity measurement, suggesting that the evaporation effect can be ignored.

The measured viscosity of liquid ZrO<sub>2</sub> is shown in Fig. 9. Because there are no literature data of experimentally obtained viscosities for ZrO<sub>2</sub>, computationally calculated data based on molecular dynamics simulation [20, 21] are shown in the figure together with the present data. The data presented here are slightly higher than the calculated data. Both show more or less the same temperature dependencies. This shows that the interatomic potential used relatively well captures the energetics and might have to be modified to match the exact experimentally determined values.

In moderate ranges of temperature, the temperature-dependent viscosity of liquids can be well expressed by the Andrade equation [24].

$$\eta = \eta_0 \exp\left(\frac{E}{RT}\right) \quad (8)$$

where R is the gas constant,  $\eta_0$  is the parameter depending on the materials, and E is the activation energy for viscous flow. The data are well fitted by this Andrade equation, as shown in Fig. 9, of which functional form is given by

$$\eta_{l-ZrO_2} = (0.96 \pm 0.69) \times \exp\left\{\frac{(6.4 \pm 2.0) \times 10^4}{RT}\right\} \left(\text{mPas}\right) \left(3170 \text{ K} < T < 3471 \text{ K}\right) \quad (9)$$

where  $\eta_{l-ZrO_2}$  is the viscosity of liquid ZrO<sub>2</sub>. The deviation of the parameters in Eq. (9) is large. In order to obtain fitting parameters with smaller deviations, it is necessary to measure the viscosity at a much wider temperature range because that value is related to the temperature dependence of viscosity. However, it is difficult to measure the viscosity at extremely high temperatures because of the evaporation effect, limitations on the laser power to avoid damaging the mirror or window, and so on. Thus, in this experiment, the temperature range of the measurement is too narrow to determine the fitting parameters more accurately. Using Eq. (9), the viscosity of liquid ZrO<sub>2</sub> at its melting point was calculated to be 13 mPas, which is much lower than that of liquid Al<sub>2</sub>O<sub>3</sub>, of which the value is 46 mPa at the melting point, and the activation energy of ZrO<sub>2</sub> was found to be  $(6.6 \pm 2.1) \times 10^2$  eV/atom, while the

value of Al<sub>2</sub>O<sub>3</sub> is  $(9.6 \pm 2.1) \times 10^2$  eV/atom.

#### 4. Conclusions

The density and viscosity of liquid ZrO<sub>2</sub> were measured using an ADL furnace built at Osaka University. This novel setup was successfully verified by comparative experiments on liquid Al<sub>2</sub>O<sub>3</sub> samples. Good agreement was found for both density and viscosity with previously recorded data. The density of liquid ZrO<sub>2</sub> was calculated based on the mass and volume of the sample, within a temperature range from 2753 K to 3273 K. The density of liquid ZrO<sub>2</sub> was found to be around 4.7 g/cm<sup>3</sup> at its melting point of 2988 K and decreased linearly with increasing temperature. The viscosity of liquid ZrO<sub>2</sub> was determined applying the droplet oscillation method for temperatures in the range of 3170 K–3471 K. The viscosity of liquid ZrO<sub>2</sub> is about 13 mPa at its melting point of 2988 K. The data are well fitted by the Andrade equation with an activation energy of  $64 \pm 20$  kJ/mol. The viscosity of liquid ZrO<sub>2</sub> at its melting point is about a factor three lower than for Al<sub>2</sub>O<sub>3</sub> at its melting point. A comparison with MD simulation data showed a good agreement in terms of the temperature dependence but a slightly higher value in experiment compared with the simulation. In summary, the present work delivers the first report on the experimentally evaluated viscosities of liquid ZrO<sub>2</sub>.

#### Declarations

##### Author contribution statement

T. Kondo: Performed the experiments; Wrote the paper.

H. Muta & K. Kurosaki: Analyzed and interpreted the data; Wrote the paper.

F. Kargl: Analyzed and interpreted the data; Contributed reagents, materials, analysis tools or data.

A. Yamaji & M. Furuya: Analyzed and interpreted the data.

Y. Ohishi: Conceived and designed the experiments; Wrote the paper.

##### Funding statement

A part of this study is the result of "Deepening Understanding of Ex-Vessel Corium Behavior by Multi-Physics Modeling" carried out under the Strategic Promotion Program for Basic Nuclear Research by the Ministry of Education, Culture, Sports, Science and Technology of Japan. This work was also supported by a Grant-in-Aid for JSPS Fellows, 18J10057.

##### Competing interest statement

The authors declare no conflict of interest.

##### Additional information

No additional information is available for this paper.

#### References

- [1] A. Yamaji, X. Li, Development of MPS method for analyzing melt spreading behavior and MCCI in severe accidents, *J. Phys. Conf. Ser.* 739 (2016).
- [2] Y. Ohishi, H. Muta, K. Kurosaki, J.T. Okada, T. Ishikawa, Y. Watanabe, S. Yamanaka, Thermophysical properties of molten core materials: Zr–Fe alloys measured by electrostatic levitation, *J. Nucl. Sci. Technol.* 53 (2016) 1943–1950.
- [3] Y. Ohishi, T. Kondo, T. Ishikawa, J.T. Okada, Y. Watanabe, H. Muta, K. Kurosaki, S. Yamanaka, Physical properties of molten core materials: Zr–Ni and Zr–Cr alloys measured by electrostatic levitation, *J. Nucl. Mater.* 485 (2016) 129–136.
- [4] S. Kohara, J. Akola, L. Patrikeev, M. Ropo, K. Ohara, M. Itou, A. Fujiwara, J. Yahiro, J.T. Okada, T. Ishikawa, A. Mizuno, Atomic and electronic structures of an extremely fragile liquid, *Nat. Commun.* 5 (2014) 1–8.
- [5] D. Cubicciotti, The melting point-composition diagram of the zirconium-oxygen system, *J. Am. Chem. Soc.* 73 (1951) 2032–2035.

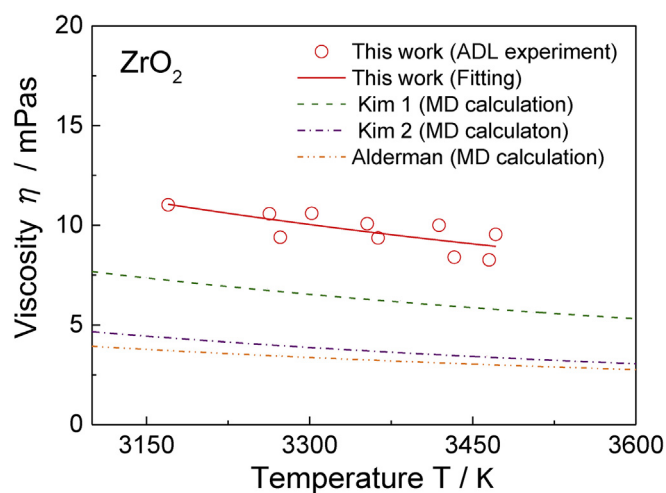


Fig. 9. Temperature dependent viscosity of liquid zirconia determined from independent runs on fresh ZrO<sub>2</sub> samples (symbols) together with a fit applying Eq. (6) (solid red line) in comparison with viscosity data determined from MD simulations by Kim et al. [17] (dashed green line).

- [6] F. Millot, J.C. Rifflet, G. Wille, High-temperature properties of liquid boron from contactless techniques 1, *Int. J. Thermophys.* 23 (2002) 1185–1195.
- [7] D. Langstaff, M. Gunn, G.N. Greaves, A. Marsing, F. Kargl, D. Langstaff, M. Gunn, G.N. Greaves, A. Marsing, F. Kargl, Aerodynamic levitator furnace for measuring thermophysical properties of refractory liquids Aerodynamic levitator furnace for measuring thermophysical properties, *Rev. Sci. Instrum.* 84 (2013) 124901.
- [8] Y. Ohishi, F. Kargl, F. Nakamori, H. Muta, K. Kurosaki, S. Yamanaka, Physical properties of core-concrete systems: Al<sub>2</sub>O<sub>3</sub>-ZrO<sub>2</sub> molten materials measured by aerodynamic levitation, *J. Nucl. Mater.* 487 (2017) 121–127.
- [9] F. Kargl, C. Yuan, G.N. Greaves, Aerodynamic Levitation: thermophysical property measurements of liquid oxides, *Int. J. Microgravity Sci. Appl.* 32 (2015) 1–5.
- [10] S. Krishnan, G.P. Hansen, R.H. Hauge, J.L. Margrave, Spectral emissivities and optical properties of electromagnetically levitated liquid metals as functions of temperature and wavelength, *High Temp. Sci.* 29 (1990) 17.
- [11] H. Lamb, On the oscillations of a viscous spheroid, *Proc. Lond. Math. Soc.* (1881) 51.
- [12] H. Tamaru, T. Takada, C. Koyama, H. Saruwatari, Y. Nakamura, T. Ishikawa, Status of the electrostatic levitation furnace (ELF) in the ISS-KIBO, *Microgravity Sci. Technol.* (2018) 643–651.
- [13] P.F. Paradis, T. Ishikawa, Y. Saita, S. Yoda, Non-contact thermophysical property measurements of liquid and undercooled alumina, *Jpn. J. Appl. Phys.* 43 (2004) 1496–1500.
- [14] A.D. Kirshenbaum, J.A. Cahill, The density of liquid aluminium oxide, *J. Inorg. Nucl. Chem.* 14 (1960) 283–287.
- [15] P.F. Paradis, T. Ishikawa, Surface tension and viscosity measurements of liquid and undercooled alumina by containerless techniques, *Japanese J. Appl. Physics, Part 1 Regul. Pap. Short Notes Rev. Pap.* 44 (2005) 5082–5085.
- [16] V.P. Elyutin, B.C. Mitin, Y.A. Nagibin, Properties of liquid aluminum oxide, *Fiz. Aerodispersnik. Sisk.* 7 (1972) 104.
- [17] J.L. Bates, C.E. Mcneilly, J.J. Rasmussen, Properties of molten ceramics, *Ceram. Sev. Environ.* 5 (1971) 11–26.
- [18] G. Urbain, Viscosity of liquid alumina, *Rev. Int. Hautes Temper. Refract. Fr.* 19 (1982) 55.
- [19] D. Grishchenko, P. Piluso, Recent progress in the gas-film levitation as a method for thermophysical properties measurement: applicator to ZrO<sub>2</sub>-Al<sub>2</sub>O<sub>3</sub> system, *High. Temp. – High. Press.* 40 (2010) 127–149.
- [20] W.K. Kim, J.H. Shim, M. Kaviany, Thermophysical properties of liquid UO<sub>2</sub>, ZrO<sub>2</sub> and corium by molecular dynamics and predictive models, *J. Nucl. Mater.* 491 (2017) 126–137.
- [21] O.L.G. Alderman, C.J. Benmore, J.K.R. Weber, L.B. Skinner, A.J. Tamalonis, S. Sendelbach, A. Hebden, M.A. Williamson, Corium lavas: structure and properties of molten UO<sub>2</sub>-ZrO<sub>2</sub> under meltdown conditions, *Sci. Rep.* 8 (2018) 2–11.
- [22] V.G. Asmolov, V.N. Zagryazkin, E.V. Astakhova, V.Y. Vishnevskii, The density of UO<sub>2</sub> – ZrO<sub>2</sub> alloys, *High Temp.* 41 (2003) 714–719.
- [23] S.J. McCormack, A. Tamalonis, R.J.K. Weber, W.M. Kriven, Temperature gradients for thermophysical and thermochemical property measurements to 3000 °C for an aerodynamically levitated spheroid Temperature gradients for thermophysical and thermochemical property measurements to 3000 °C for an aerodynamically le, *Rev. Sci. Instrum.* 90 (2019) 1–10.
- [24] T. Iida, R.T.L. Guthrie, *The Physical Properties of Liquid Metals*, Oxford Science Publication, 1988.